

Multi-Objective Calibration of Nonlinear Muskingum Model Using Non-Dominated Sorting Genetic Algorithm-II

Jungang Luo^{1,2,*}, Xiao Zhang² and Xuan Zhang²

¹State Key Laboratory Base of Eco-hydraulic Engineering in Arid Area, Xi'an University of Technology, Xi'an, China

²Institute of Water Resources and Hydro-Electric Engineering, Xi'an University of Technology, Xi'an, China

*Corresponding author

Abstract—Parameter calibration of hydrological model is one of the most important issues in the field of hydrology. Practice experience suggests that the traditional calibration of hydrological model with single objective cannot properly measure all of the behaviors of hydrological system. In order to successfully calibrate a hydrological model, multiple criteria should be considered. In this study, an multi-objective calibration routine of Muskingum model is developed using the Non-dominated Sorting Genetic Algorithm II (NSGA-II). The performance of the multi-objective calibration procedure is authenticated by three cases involving single-peak, multi-peak, and non-smooth hydrographs. The results show that the multi-objective calibration procedure is consistent and effective in estimating parameters of the Muskingum model.

keywords-muskingum model; multi-objective optimization; nsga-ii; parameter estimation

I. INTRODUCTION

The Muskingum model is the most widely used and efficient method for flood routing in hydrologic engineering. Parameters estimation of Muskingum model is very significant in both exploitation and utilization of water resources and hydrological forecasting. There are a variety of techniques for estimating the parameters of the Muskingum model for flood routing, such as least squares method (LSM) [1], Hook-Jeeve (HJ) pattern search technique in combination with simple linear regression (LR) [2], nonlinear least-squares regression (NONLR) technique [3], genetic algorithm (GA) [4], harmony search (HS) algorithm [5], dual formulation method [6], Broyden-Fletcher-Goldfarb-Shanno (BFGS) technique [7], approximate methods [8], chance-constrained optimization approach [9], particles warm optimization (PSO) algorithm [10], immune clonal selection algorithm (ICSA) [11], Nelder-Mead Simplex (NMS) algorithm [12], parameter-setting-free technique interfaced with a harmony search (PSF-HS) algorithm [13], differential evolution (DE) algorithm [14], hybrid harmony search algorithm (HS-BFGS) [15], spreadsheet software [16], hybrid particle swarm optimization (HPSO)[17], new discretization methods [18], adaptive hybrid particle swarm optimization (AHPSO) [19].

In all of these method, the calibration procedure is based on a single performance metric or calibration criterion. The main objective of this study is to perform calibration of the

Muskingum using multi-objective optimization technique. In this study, a multi-objective evolutionary algorithm known as Non-dominated Sorting Genetic Algorithm II (NSGA-II), has been used to develop an automatic calibration routine for Muskingum model. The performance of the multi-objective calibration procedure is authenticated by three cases involving single-peak, multi-peak, and non-smooth hydrographs.

II. NONLINEAR MUSKINGUM MODEL

The Muskingum models fall under the category of lumped flood routing methods that use the continuity equation

$$\frac{dS_t}{dt} = I_t - O_t \quad (1)$$

Where S_t , I_t and O_t are the simultaneous amounts of storage, inflow and outflow respectively at time t . If storage is linearly related to inflow and outflow, the linear form Muskingum model can be expressed as

$$S_t = K[xI_t + (1-x)O_t] \quad (2)$$

where K is the storage-time constant; x is the weighting factor. If the relationship between $[xI_t + (1-x)O_t]$ and S_t is nonlinear, use of the nonlinear Muskingum model is considered more appropriate. The nonlinear form of Muskingum model can be expressed as

$$S_t = K[xI_t + (1-x)O_t]^m \quad (3)$$

In which, m is an exponent that define the nonlinear relationship between weighted flow and accumulated storage. To calibrate the parameters K , x and m of the nonlinear Muskingum model, the routing procedure can be made as following.

By rearranging Eq. (3), the rate of outflow O_t can be achieved as

$$O_t = \left(\frac{1}{1-x} \right) \left(\frac{S_t}{K} \right)^{1/m} - \left(\frac{x}{1-x} \right) I_t \quad (4)$$

Combining Eq. (4) and Eq. (1), the state equation can be expressed as

$$\frac{\Delta S_t}{\Delta t} = - \left(\frac{1}{1-x} \right) \left(\frac{S_t}{K} \right)^{1/m} + \left(\frac{1}{1-x} \right) I_t \quad (5)$$

The next accumulated storage can be obtained as

$$S_{t+1} = S_t + \Delta S_t \quad (6)$$

The next outflow in Eq.(3) can be calculated as

$$O_{t+1} = \left(\frac{1}{1-x} \right) \left(\frac{S_{t+1}}{K} \right)^{1/m} - \left(\frac{x}{1-x} \right) I_t \quad (7)$$

The solution procedure for the nonlinear model of Eq. (3) includes the following steps:

Step 1: Assume values for three model parameters K , x and m .

Step 2: Calculate the storage S_t using Eq. (3), where initial outflow is the same as initial inflow $Q_0 = I_0$.

Step 3: Calculate the time rate of change of storage volume using Eq. (5).

Step 4: Estimate the next storage S_{t+1} using Eq. (6).

Step 5: Calculate the next outflow O_{t+1} using Eq. (7).

Step 6: Repeat Steps 3 to 5 for the following time intervals.

III. MULTI-OBJECTIVE CALIBRATION USING NSGA-II

A. Formulation of Multi-objective Calibration Problem

In model calibration, the match of measured data to simulated values is one of the most important indicators of how well a model is calibrated. To calibrate a model with multiple variables included in the calibration, model parameters are adjusted so that satisfactory agreements between the measurements and simulations for all variables included in calibration are achieved simultaneously. Hence to calibrate a model is to solve a multi-objective optimization problem, which can be described mathematically as follows:

$$\begin{aligned} \text{Minimize} \quad & \mathbf{F}(\mathbf{x}) = \{f_1(\mathbf{x}), f_2(\mathbf{x}), \dots, f_M(\mathbf{x})\} \\ \text{Subject to} \quad & \mathbf{x}_{\text{low}} \leq \mathbf{x} \leq \mathbf{x}_{\text{up}} \end{aligned} \quad (8)$$

where $\mathbf{x} = (x_1, x_2, \dots, x_N)$ is the parameter vector and N is the number of parameters to be calibrated; \mathbf{x}_{low} and \mathbf{x}_{up} represent the sets of lower and upper bounds of parameters; $\mathbf{F}(\mathbf{x})$ is the vector of objective functions, $f_1(\mathbf{x}), f_2(\mathbf{x}), \dots, f_M(\mathbf{x})$; M is the total number of objective functions.

B. Non-dominated Sorting Genetic Algorithm

The Non-dominated sorting genetic algorithm (NSGA-II) is an outstanding multi-objective optimizer base on evolutionary computation which is a nature inspired computational intelligence technique. By evolving a population of solutions simultaneously, NSGA-II can obtain a required set of non-dominated solutions in a single run, and thus provide the decision makers with more comprehensive information about the target multi-objective optimization problem. NSGA-II maintains a population of solutions with determined size and evolves the individuals in the population to enhance their quality. At each iteration of the evolutionary procedure, the individuals with lower non-dominate rank and less density level will be selected to survive and proliferate. During iterations, the qualities of the individuals in the population gradually improves. As a consequence, the best trade-offs are finally obtained. The workflow of NSGA-II can be described as follows.

Step 1: Create a random parent population of size N .

Step 2: Sort the population based on the non-domination.

Step 3: Assign each solution a fitness (or rank) equal to its non-domination level (minimisation of fitness is assumed).

Step 4: Use the usual binary tournament selection, recombination, and mutation operators to create a new offspring population of size N .

Step 5: Combine the offspring and parent population to form extended population of size $2N$.

Step 6: Sort the extended population based on non-domination.

Step 7: Fill new population of size N with the individuals from the sorting fronts starting from the best.

Step 8: Invoke the crowding comparison operator to ensure diversity if a front can only partially fill the next generation (this strategy is called ‘‘niching’’).

Step 9: Repeat the steps 2 to 8 until the stopping criterion is met. The stopping criterion may be a specified number of generations.

IV. CALIBRATION CRITERIA

A. Objective Function

Some studies indicated that the success of a calibration process is highly dependent on the objective function chosen as a calibration criterion [20, 21]. The most commonly used calibration criterion is the sum of squared errors between observed and simulated model responses [21]. In order to

obtain a successful calibration by using automatic optimization routines, it is necessary to formulate the calibration objectives. In this study, two objective function formulate as follow:

1. Sum of the square of the deviations between the routed and observed outflows (SSQ)

$$f_1(\theta) = \sum_{t=1}^N [O_{obs,t} - O_{sim,t}(\theta)]^2 \quad (9)$$

2. Deviations of peak of routed and actual outflows (DPO)

$$f_2(\theta) = \sum_{i=1}^L |O_{obs,i}^{peak} - O_{sim,i}^{peak}(\theta)| \quad (10)$$

Where $O_{obs,t}$ and $O_{sim,t}$ are the observed and routed outflow at time t , respectively. N is the total number of time steps in the calibration period. θ is the set of model parameters to be calibrated. $O_{obs,i}^{peak}$ and $O_{sim,i}^{peak}$ are the observed and routed maximum outflow at peak flow event no. i , respectively. L is the number of peak flow events.

B. Performance Evaluation Criteria

The performance of the multi-objective calibration method is evaluated by two goodness-of-fit measures, namely the root mean square error (RMSE) and the coefficient of efficiency (CE).

The RMSE is expressed as

$$RMSE = \sqrt{\frac{1}{N} \sum_{t=1}^N (O_{obs,t} - O_{sim,t})^2} \quad (11)$$

The coefficient of efficiency, which has been widely used to evaluate performances of hydrologic models, is used to measure the goodness-of-fit [21]. Nash and Sutcliffe (1970) defined the coefficient of efficiency as

$$CE = 1 - \frac{\sum_{t=1}^N (O_{obs,t} - O_{sim,t})^2}{\sum_{t=1}^N (O_{obs,t} - \bar{O}_{obs})^2} \quad (12)$$

where \bar{O}_{obs} is the average observed outflow.

V. APPLICATION EXAMPLE

A. Example 1: Single Peak Hydrograph

This example uses the data set of Wison (1974). The data set is a typical single-peak flood hydrograph and extensively used to test various parameter estimation approaches. In this

example, the Muskingum model is calibrated by NSGA-II algorithm based on two objectives, the SSQ and DPO. The Pareto front for the calibration of sum of the square of the deviations and peak deviations between the routed and observed outflows is shown in Figure 1. The figure illustrate significant trade-off between SSQ and DPO, i.e. a parameter set that gives good calibration of overall agreement results in bad calibration of peak flow, and vice versa. Thus, by moving from A1 to C1 along the Pareto front, a reduction of the deviations of peak of routed and actual outflows is obtained at the expense of an increase in the sum of the square of the deviations between the routed and observed outflows. The minimum SSQ of 36.77 (corresponding to RMSE=1.29, CE=1.00) at the solution of point A1 increases to 41.38 (RMSE=1.37, CE=1.00) at the solution of point C1. At the same times, the DPO is reduced from 0.90 at the point of A1 with minimum SSQ to 0 at the point of C1.

The solutions along the Pareto front are equally optimal as far as the calibration routine is concerned; however, a decision maker can choose one specific solution based on the importance of the calibration criteria, i.e., it merely depends on the type of model application [21]. In practices, the trade-off solution, which make compromised between the two objectives, is shown as B1 in Figure 1. The resulting DPO value is 0.39 showing significant improvement over DPO value obtained using default simulation from single-objective calibration under almost the same RMSE and CE. The values of performance criteria are presented in Table 1. Graphical comparison between observed and simulated outflow for the solutions are shown in Figure 2. As is shown in Figure 2, the plots depict that the routed outflow hydrograph, using the trade-off solution (Point B1) obtained from multi-objective calibration, is closer to the observed outflow hydrograph at peak flow than the simulated outflow hydrograph of the parameters estimated from single-objective calibration.

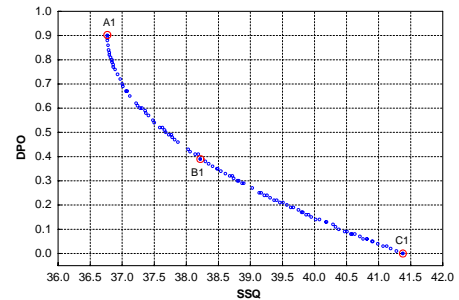


FIGURE I. PARETO FRONTS FOR SINGLE-PEAKED OUTFLOW HYDROGRAPH

TABLE I. COMPARISON BETWEEN SINGLE-OBJECTIVE AND MULTI-OBJECTIVE FOR SINGLE-PEAKED OUTFLOW HYDROGRAPH

Evaluation criteria	Single-objective (SSQ)	Multi-objective (SSQ +DPO)		
		A1	B1	C1
SSQ	36.77	36.77	38.22	41.38
DPO	0.90	0.90	0.39	0
RMSE	1.29	1.29	1.32	1.37
CE	1.00	1.00	1.00	1.00

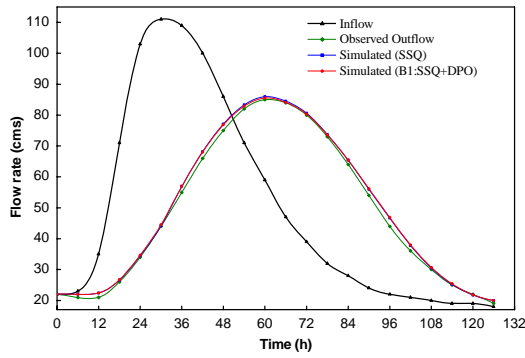


FIGURE II. COMPARISON OF SINGLE-OBJECT AND MULTI-OBJECT SIMULATED OUTFLOW FOR SINGLE-PEAKED OUTFLOW HYDROGRAPH

B. Example 2: Multi-Peak Hydrograph

This example uses the data of Viessman and Lewis (2003) presented by Al-Humoud and Esen [8]. The data set is a multi-peak flood hydrograph and have been used to test the performance of parameter estimation approaches for Muskingum model [22]. The Pareto front produced by the NSGA-II for multi-peak hydrograph is shown in Figure 3. It is clear from Figure 3 that a significant trade-off exists between the two objectives. A large reduction of the DPO with a large increase is observed when moving from A2 to C2 along the Pareto front. Table 2 presents the values of performance criteria for the solutions obtained from single-objective and multi-objective calibration. As is shown in Table 2, The minimum SSQ of 73509.62 (corresponding to RMSE=55.34, CE=0.98) at the solution of point A2 increases to 82297.74 (RMSE=58.56, CE=0.98) at the solution of point C2. At the same times, the DPO is reduced from 48.84 at the point of A2 with minimum SSQ to 0 at the point of C2. The compromise solution (Point B2) resulting DPO value is 20.33 showing significant improvement over DPO value obtained using optimal simulation from single-objective calibration. The DPO value of the compromise solution (Point B2) is 20.33, showing significant improvement over DPO value obtained from the optimal solution of single-objective calibration. The simulated outflow hydrographs along with the observed inflow and outflow hydrographs are shown in Figure 4. It is clear that the peak flows of simulated outflow hydrograph obtained from the compromise solution (Point B2) are closer to the observed peaks flow than the optimal solution of the single-objective.

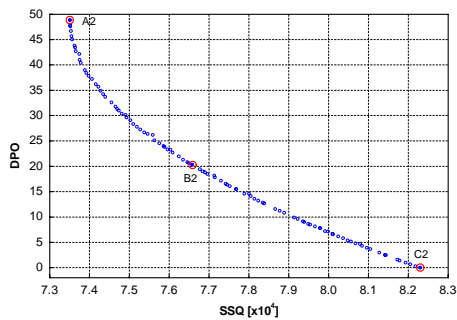


FIGURE III. PARETO FRONTS FOR MULTI-PEAKED OUTFLOW HYDROGRAPH

TABLE II. COMPARISON BETWEEN SINGLE-OBJECTIVE AND MULTI-OBJECTIVE FOR MULTI-PEAKED OUTFLOW HYDROGRAPH

Evaluation criteria	Single-objective (SSQ)	Multi-objective (SSQ +DPO)		
		A2	B2	C2
SSQ	73509.61	73509.62	76575.10	82297.74
DPO	48.82	48.84	20.33	0
RMSE	55.34	55.34	56.49	58.56
CE	0.98	0.98	0.98	0.98

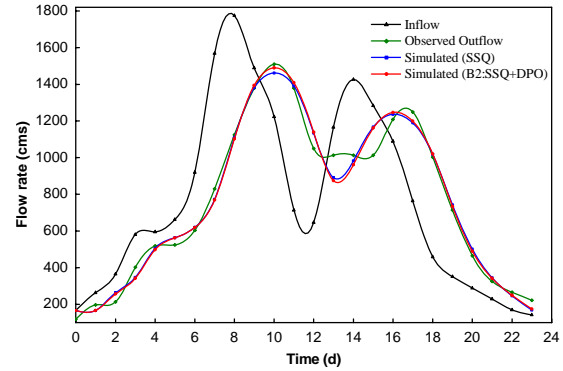


FIGURE IV. COMPARISON OF SINGLE-OBJECT AND MULTI-OBJECT SIMULATED OUTFLOW FOR MULTI-PEAKED OUTFLOW HYDROGRAPH

C. Example 3: Non-Smooth Hydrograph

This example uses the data of the River Wye stretch in the United Kingdom presented by Karahan et al [15]. Figure 5 shows the Pareto front generated by the NSGA-II for non-smooth hydrograph. It can be seen that a significant trade-off exists between the two objectives. The remarkably reduction of the DPO with a significant increase is observed when moving from A3 to C3 along the Pareto front. The minimum SSQ of 37944.16 (corresponding to RMSE=33.41, CE=0.98) at the solution of point A3 increases to 56605.36 (RMSE=40.80, CE=0.97) at the solution of point C3. At the same times, the DPO is reduced from 97.82 at the point of A3 with minimum SSQ to 0 at the point of C3. The trade-off solution, which make compromised between the two objectives, is shown as B3 in Figure 5. Table 3 presents the values of performance criteria for the solutions obtained from single-objective and multi-objective calibration. It is clear from Table 3 that the DPO value (43.68) of the compromise solution is reduced 55% compared with the optimal solution of single-objective calibration. Graphical comparison between observed and simulated outflow for the solutions are shown in Figure 6.

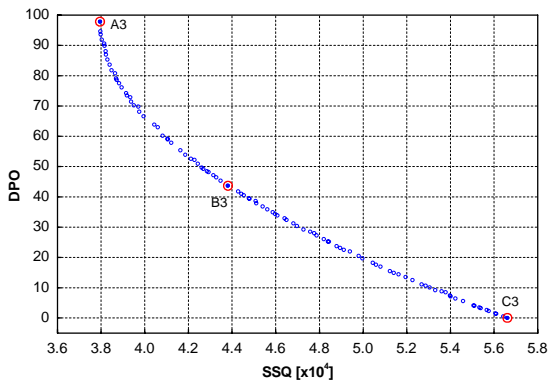


FIGURE V. PARETO FRONTS FOR NON-SMOOTH OUTFLOW HYDROGRAPH

TABLE III. COMPARISON BETWEEN SINGLE-OBJECTIVE AND MULTI-OBJECTIVE FOR NON-SMOOTH OUTFLOW HYDROGRAPH

Evaluation criteria	Single-objective (SSQ)	Multi-objective (SSQ +DPO)		
		A3	B3	C3
SSQ	37944.15	37944.16	43807.86	56605.36
DPO	97.84	97.82	43.68	0
RMSE	33.41	33.41	35.90	40.80
CE	0.98	0.98	0.97	0.97

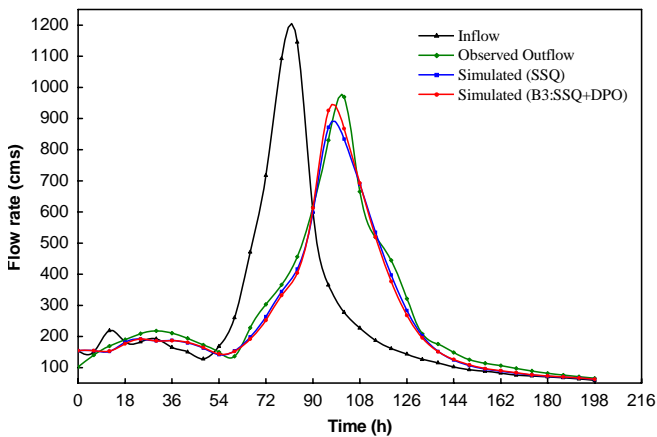


FIGURE VI. COMPARISON OF SINGLE OBJECT AND MULTI-OBJECT SIMULATED OUTFLOW FOR NON-SMOOTH OUTFLOW HYDROGRAPH

VI. CONCLUSIONS

Parameter calibration of Muskingum model based on a single objective is often inadequate to measure properly the simulation of all the important characteristics of flood routing. In this paper, an multi-objective automatic calibration approach for the nonlinear Muskingum has been developed using a multi-objective evolutionary algorithm known as NSGA-II. The two calibration objectives have been considered in the calibration procedure of Muskingum model: (1) sum of the square of the deviations between the routed and observed outflows (SSQ), and (2) deviations of peak of routed and actual outflows (DPO). The three application examples demonstrated that significant

trade-off between the two objectives exist, implying that no unique single solution is able to optimize all two objectives simultaneously. Instead, the solution to the calibration problem is given as a set of Pareto optimal solution. Thus, it allows the user to choose a particular solution based on the importance of the calibration criteria involved. The results of three examples clearly showed that the multi-objective automatic calibration approach is consistent and effective in estimating parameters of the nonlinear Muskingum model.

ACKNOWLEDGMENT

This work was supported by the National Natural Science Foundation of China under Grant Nos. 51109175 and 61303119, the Science and Technology Program of Shaanxi Province under Grant Nos. 2014K09-07 and 2015KJXX-30, the National Research Foundation for the Doctoral Program of Higher Education of China under Grant No. 20126118110011.

REFERENCES

- [1] Gill, M.A., Flood routing by the Muskingum method. *Journal of Hydrology*, 1978, 36(3-4): 353-363.
- [2] Tung, Y.K., River Flood Routing by Nonlinear Muskingum Method. *Journal of Hydraulic Engineering*, 1985, 111(12): 1447-1460.
- [3] Yoon, J. and G. Padmanabhan, Parameter Estimation of Linear and Nonlinear Muskingum Models. *Journal of Water Resources Planning and Management*, 1993, 119(5): 600-610.
- [4] Mohan, S., Parameter Estimation of Nonlinear Muskingum Models Using Genetic Algorithm. *Journal of Hydraulic Engineering*, 1997, 123(2): 137-142.
- [5] Kim, J.H., Z.W. Geem, and E.S. Kim, Parameter estimation of the nonlinear muskingum model using harmony search. *JAWRA Journal of the American Water Resources Association*, 2001, 37(5): 1131-1138.
- [6] Das, A., Parameter Estimation for Muskingum Models. *Journal of Irrigation and Drainage Engineering*, 2004, 130(2): 140-147.
- [7] Geem, Z.W., Parameter Estimation for the Nonlinear Muskingum Model Using the BFGS Technique. *Journal of Irrigation and Drainage Engineering*, 2006, 132(5): 474-478.
- [8] Al-Humoud, J. and I. Esen, Approximate Methods for the Estimation of Muskingum Flood Routing Parameters. *Water Resources Management*, 2006, 20(6): 979-990.
- [9] Das, A., Chance-Constrained Optimization-Based Parameter Estimation for Muskingum Models. *Journal of Irrigation and Drainage Engineering*, 2007, 133(5): 487-494.
- [10] Chu, H.J. and L.C. Chang, Applying Particle Swarm Optimization to Parameter Estimation of the Nonlinear Muskingum Model. *Journal of Hydrologic Engineering*, 2009, 14(9): 1024-1027.
- [11] Luo, J. and J. Xie, Parameter Estimation for Nonlinear Muskingum Model Based on Immune Clonal Selection Algorithm. *Journal of Hydrologic Engineering*, 2010, 15(10): 844-851.
- [12] Barati, R., Parameter Estimation of Nonlinear Muskingum Models Using Nelder-Mead Simplex Algorithm. *Journal of Hydrologic Engineering*, 2011, 16(11): 946-954.
- [13] Geem, Z.W., Parameter Estimation of the Nonlinear Muskingum Model Using Parameter-Setting-Free Harmony Search. *Journal of Hydrologic Engineering*, 2011, 16(8): 684-688.
- [14] Xu, D., L. Qiu, and S. Chen, Estimation of Nonlinear Muskingum Model Parameter Using Differential Evolution. *Journal of Hydrologic Engineering*, 2012, 17(2): 348-353.
- [15] Karahan, H., G. Gurarslan, and Z.W. Geem, Parameter Estimation of the Nonlinear Muskingum Flood-Routing Model Using a Hybrid Harmony Search Algorithm. *Journal of Hydrologic Engineering*, 2013, 18(3): 352-360.

- [16] Barati, R., Application of excel solver for parameter estimation of the nonlinear Muskingum models. *Ksce Journal of Civil Engineering*, 2013, 17(5): 1139-1148.
- [17] Ouyang, A.J., et al., Hybrid particle swarm optimization for parameter estimation of Muskingum model. *Neural Computing & Applications*, 2014, 25(7-8): 1785-1799.
- [18] Sheng, Z., et al., A Novel Parameter Estimation Method for Muskingum Model Using New Newton-Type Trust Region Algorithm. *Mathematical Problems in Engineering*, 2014, 2014: 1-7.
- [19] Ouyang, A.J., Z. Tang, and K.L. Li, Estimating parameters of muskingum model using an adaptive hybrid pso algorithm. *International Journal of Pattern Recognition and Artificial Intelligence*, 2014, 28(1): 178-215.
- [20] Gupta, H.V., S. Sorooshian, and P.O. Yapo, Toward improved calibration of hydrologic models: Multiple and noncommensurable measures of information. *Water Resources Research*, 1998, 34(4): 751-763.
- [21] Bekele, E.G. and J.W. Nicklow, Multi-objective automatic calibration of SWAT using NSGA-II. *Journal of Hydrology*, 2007, 341(3-4): 165-176.
- [22] Easa, S., Improved Nonlinear Muskingum Model with Variable Exponent Parameter. *Journal of Hydrologic Engineering*, 2013, 18(12): 1790-1794.